# Exploration of the combined vibration parameters and external magnetic field in diagnosing asynchronous electric motors

*Matkarim* Ibragimov[1], *Dilmurod* Akbarov[1*], *Tajiddin* Toshev[2], *Kholiyor Sayyid* Safarov[2] and *Oliyaxon* Zayniyeva[2]

[1]Department Electrical Technology and Using of Electrical Equipment, “Tashkent Institute of Irrigation and Agricultural Mechanization Engineers” National Research University, 100000 Tashkent, Uzbekistan
[2]Department of Electrical Engineering, Karshi Engineering and Economics Institute, 180100 Karshi, Uzbekistan

**Abstract.** This paper presents the results of the development and application of a software-hardware complex for assessing the vibration level and external magnetic field intensity of asynchronous electric motors with the aim of diagnosing emerging defects. The issues of increasing the reliability and durability of asynchronous electric motors, as the most critical components in technological equipment complexes, are of utmost importance. Theoretical calculations describing the relationship between changes in the intensity of the external magnetic field and the presence of defects in asynchronous electric motors were conducted. Experimental measurements were performed using a compact portable device developed by the authors, equipped with a built-in Hall sensor. Experiments to determine the parameters of the external magnetic field were conducted on several types of electric motors, for which preliminary vibration measurements were conducted. Based on the results of vibration analysis and the distribution of the external magnetic field of the motor, a detailed list of defects detectable using this comprehensive diagnostic method has been compiled.

## 1. Introduction

In the Republic of Uzbekistan, the cotton raw material processing industry holds significant importance within the agricultural sector. With 145 cotton-textile clusters, over 250 cotton receiving points, and more than 21 self-employed enterprises, the cotton ginning industry plays a vital role in the country. The industry operates a wide range of equipment, including approximately 60,000 conditional units, over 160 power transformers, and more than 75,000 electric motors of varying capacities. Notably, nearly 95% of these motors are asynchronous electric motors [1].

Due to their simple and technologically advanced design, high energy efficiency, operational reliability, and resistance to overloads, asynchronous motors are widely used in the agricultural and industrial complex. They find applications in various sectors such as transportation, machinery drives, pumps, fans, compressors, and lifting mechanisms. Therefore, the issues of increasing the reliability and durability of asynchronous motors, as the most critical components in technological equipment complexes, are of utmost importance.

The assessment of the technical condition of electric machines is an important task that allows for the early detection of emerging defects and helps prevent potentially serious negative consequences. Therefore, the development of inexpensive, user-friendly, and accurate methods for monitoring and diagnosing the condition of electric motors is crucial. The most effective methods for this purpose include vibration diagnostics [2-3], thermal monitoring [4-5], and analysis of external magnetic field (EMF) parameters of electric machines [6].

Vibration diagnostics is particularly effective in detecting most mechanical and some electrical defects, while thermal monitoring can identify defects related to overheating. In the future, monitoring EMF parameters will enable the detection of electrical defects in electric motors [7]. These methods complement each other well, as they are based on the measurement and analysis of phenomena with different physical characteristics. The development of these methods will allow for a comprehensive assessment of the technical condition of electric motors and increase the reliability of defect diagnosis [8].

*Corresponding author: uzigabek1920@mail.ru

## 2. Methods

In this study, we explore the method of controlling and analyzing the parameters of the external magnetic field to diagnose emerging defects in asynchronous electric motors. As per theoretical principles, the overall rotating magnetic field generated by three-phase alternating current electric machines can be decomposed into two magnetic moment components along mutually perpendicular directions within the main plane of the machine [9].

$$M_{MX} = 0; \qquad M_{MY} = M_M \cos(\omega \cdot t + \varphi_M); \qquad M_{MZ} = M_M \sin(\omega \cdot t + \varphi_M); \qquad (1)$$

Here, $M_M$, $\omega$, and $\varphi_M$ represent the amplitude, frequency, and phase of the magnetic moment, respectively.
Let's consider the projection of the external magnetic field (EMF) onto one of the axes, such as the Z-axis [10]. The current value of the magnetic induction in the air gap of the machine can be expressed as:

$$B_\varphi = F_\varphi \cdot \lambda_\varphi; \qquad (2)$$

Here, $F\varphi$ and $\lambda\varphi$ represent the current values of the magnetic force and magnetic permeability in the air gap.
In the case of symmetrical arrangement of the rotor with respect to the stator, we obtain [9]:

$$\lambda_\varphi = \lambda_0 = \frac{\mu_0}{\kappa_\mu \cdot \kappa_\delta \cdot \delta_0} \qquad (3)$$

Here, $\kappa_\delta$ -is the air gap coefficient (Carter's coefficient), $\kappa_\mu$ -is the coefficient that accounts for the saturation of the tooth zone, $\delta_0$ -is the air gap distance between the rotor and stator, and μ0 is the magnetic permeability constant.
The fundamental harmonic of the magnetizing force in the alternating current machine can be expressed as:

$$F_\varphi = F_0 \cos(\omega \cdot t + p \cdot \varphi) \qquad (4)$$

Here; ω is the frequency of the stator's magnetic field rotation.
We obtain the expression:

$$B = B_m cos(\omega \cdot t + p \cdot \varphi) \qquad (5)$$

Here; $B_m = F_m \cdot \lambda_0$ is the amplitude of the fundamental harmonic of the magnetic induction for a symmetrical air gap. The presence of a spectrum of harmonics in the magnetic induction in the air gap leads to the appearance of a similar spectrum in the external magnetic field of the machine. The induction of the external magnetic field decreases with distance from the source according to a certain law $B = 1/R^{n+2}$:
here; $n$ is the order of the magnetic harmonic. Therefore, for the fundamental external magnetic field of the machine with harmonics of order r, we can neglect the harmonics of order *(p+k)* due to their small magnitude. Since the external magnetic field of the machine is shielded by the housing, this should be taken into account, for example, by using the shielding coefficient $\kappa_e$. Then, the radial induction of the external magnetic field of the machine can be expressed as:

$$B_R = B_0 cos(\omega \cdot t + p \cdot \varphi) \qquad (6)$$

Here, $B_0 = \kappa_e \cdot B_m$.
Thus, the induction of the external magnetic field of a defect-free motor varies according to a sinusoidal law in time (Figure 1).

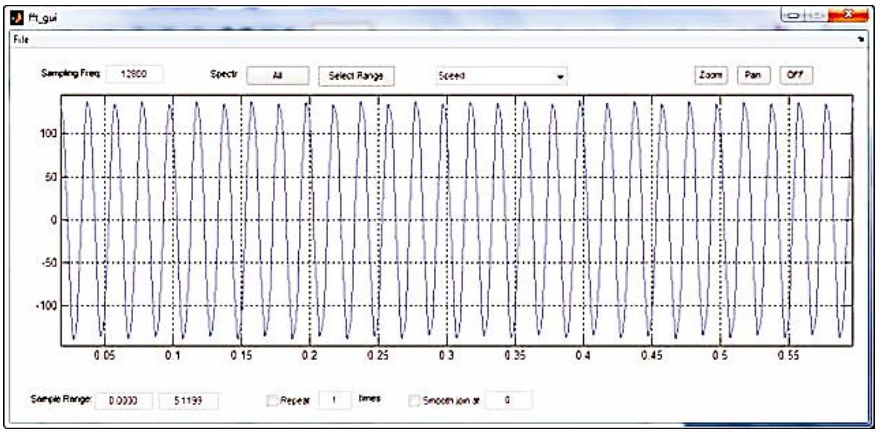


**Fig. 1.** The main working window of the "Fft_gui" program with the time signal of the external magnetic field induction of a defect-free electric motor

## 3. Solving style

Development of an External Magnetic Field Measurement Device. In order to conduct experimental measurements of the external magnetic field induction on various types of electric motors while simulating defects, a compact portable device was developed. The block diagram of the device is shown in Fig. 2.

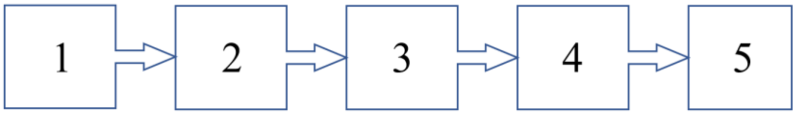


**Fig. 2.** Structural diagram of the device for measuring the external magnetic field induction: 1 - power supply; 2 - low-pass filters; 3 - Hall sensor; 4 - amplifier; 5 - digital recording block.

The power supply provides voltage to the low-pass filters with a cut-off frequency $F_{cp}$=1000 Hz, designed to filter out high-frequency components and noise from the input voltage. The filtered voltage then goes to the linear magnetic field sensor (Hall sensor). When the Hall sensor is placed in a magnetic field, the magnetic induction vector generates a potential difference in the sensor equivalent to the external magnetic field. The output voltage from the Hall sensor is then amplified by the amplifier and further fed into the input channel of the digital block. In the digital recording block, the analog signal is converted into a digital format and stored for further playback and analysis [11]. The calibration of the external magnetic field induction measurement device was conducted on a specially made test bench, which included an inductance coil, a power supply, and an ammeter. In order to determine the voltage conversion coefficient from the output of the Hall sensor to the dimension of magnetic field intensity, measurements were performed using the magnetic measuring ferroprobe device F-205.30A. The measurements were conducted using a ferroprobe converter - polemer and the developed instrument [12-13].
At the same point in the center of the coil, eight measurements were taken using the polemer, both in the positive and negative regions of the Hall sensor, in order to determine the sensitivity of each of its sides. After processing the measurement results, conversion coefficients were obtained for the positive ($K_{pU+}$) and negative ($K_{pU-}$) regions of the sensor, expressed in $\left[\frac{A/m}{v}\right]$.

$$K_{pU+} = \frac{<H_n>}{<U_+>} = \frac{232.1}{0.86} = 270\,;$$

$$K_{pU-} = \frac{<H_n>}{<U_->} = \frac{232.1}{-1.119} = -207$$

The directional diagram, showing the dependence of the output voltage on the angle α of the deviation of the sensor plane, was obtained using the calibration stand (Figure 3). Experimentally, it was determined that when the sensor plane is deviated by 20° from perpendicular to the magnetic field vector, the output signal changes by 100 mV, equivalent to 11.1%.
During the experiments, it was found that the components of the field directed along the outer circumference of the electric motor stator (Figure 4, b) provide the most informative data. Therefore, the sensor plane was oriented perpendicular to these lines of the field [14].
The measurement results were processed using a custom-made program "Fft_gui" in the MatLab programming environment, allowing the analysis of temporal signals of magnetic field intensity and the fast Fourier transform to obtain spectral characteristics.

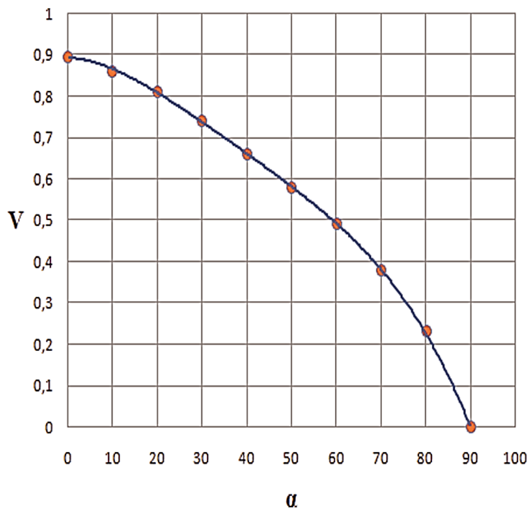


**Fig.3.** Directional Diagram

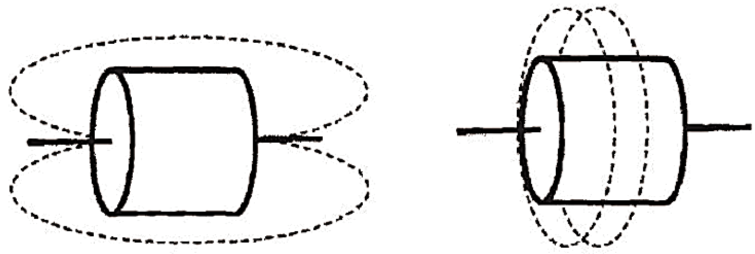

*a)* *b)*

**Fig.4.** Schematic Representation of Components of the External Magnetic Field of the Motor

The duration of the recorded signal in txt format was 5.12 seconds, which allowed obtaining a spectrum with a resolution of 0.195 Hz (reducing the recording duration would decrease the spectrum resolution and provide an incomplete picture of the harmonic composition). The main working window of the program is shown in Figure 1.

Measurement Methodology. To conduct experiments on the motor, fixed points were selected for measuring the intensity of the External Magnetic Field (EMF). The minimum number of points around the motor's stator that adequately represents the EMF distribution is eight. The number of control points can be increased, but this would increase the complexity of measurement and data processing. In the selected points, markers were placed to eliminate the possibility of inaccuracies in sensor placement.

To achieve this, signal recording was performed sequentially at each point. The circular measurement was repeated five times to reduce errors caused by imprecise sensor placement. Circular diagrams of EMF intensity were then constructed based on the averaged values of EMF amplitude.

## 4. Results and discussions

Experiments to determine the EMF parameters were conducted on several types of electric motors, for which preliminary vibration measurements were carried out. Vibration measurements and analysis were conducted using the vibration collector SK-1100 and the software "Vibroanalysis 2.52" by the company "Tekhnekon." The points and directions of motor vibration measurements are shown in Figure 5.

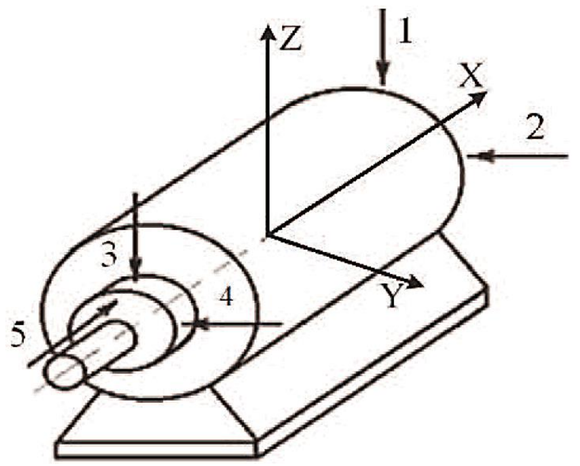


**Fig.5.** Points and Directions of Vibration Measurements on Induction Motors

The results of vibration measurements. The general level of vibration (RMS of the vibration velocity) and the preliminary diagnosis of the state according to the time signal and spectrum are presented in Table. 1.

The vibration level of motor #1 is within the normal range and corresponds to the allowable vibration for new motors (1.4 mm/s). The main contributors to the Vibration Velocity RMS Level are the residual (unbalanced during manufacturing) rotor imbalance (peak at the rotational frequency of 24.9 Hz) and small high-frequency components at bearing frequencies.

The vibration of motor #2 slightly exceeds the allowable level for a new motor but is still below the permissible operational level (2.8 mm/s). However, in the vibration spectrum, there are predominant peaks at the 2nd and 4th harmonics of the power frequency (100 Hz, 200 Hz), indicating asymmetry in the currents of the stator windings. As the main known vibration indicator of interturn short circuits is the presence of the fundamental harmonic at the double power frequency (2x$f_c$), it is possible to assume the presence of this defect at an early stage.

**Table.1.** Data of asynchronous electric motors and results of vibration measurements and diagnostics

| *№* | *Type of asynchronous electric motor, power.* | *Results of Vibration Diagnostics* | *Vibration Velocity RMS (Root Mean Square) Level, mm/s.* | | | | |
|---|---|---|---|---|---|---|---|
| | | | *p. 1* | *p. 2* | *p. 3* | *p. 4* | *p. 5* |
| 1 | AD90L4У3 2,2 kWt | Normal (New Asynchronous Electric Motor) | 0,68 | 0,94 | 1,08 | 1,20 | 1,19 |
| 2 | АИР90L4У3, 2,2 kWt | Inter-turn short circuit in the stator winding | 1,43 | 1,24 | 1,01 | 1,40 | 1,03 |
| 3 | 4A100L4У3, 4 kWt | Broken rotor bar | 5,94 | 1,78 | 1,31 | 1,78 | 4,03 |

The vibration level of motor #3 is significantly high and exceeds the allowable value (4.5 mm/s). The vibration spectrum has an unusual shape and contains a component at the rotational frequency $f_1$ - 25 Hz, along with a considerable number (20) of its harmonics. Among them, the 2nd, 3rd, and 4th harmonics of $f_1$ have the highest amplitude. It is possible to speculate that these are indications of an electrical defect - a broken rotor bar.

Indeed, one of the most common defects in asynchronous electric motors is the cracking and breaking of rotor bars, which are often designed in the form of a squirrel cage. Reliable diagnostics of this defect can prevent sudden failures and increase the drive's reliability. However, relying solely on vibration diagnostics may sometimes be insufficient to confidently identify this defect.

In the example provided earlier, the absence of a characteristic set of sidebands around the harmonics of the rotational frequency (fn) makes it challenging to confidently detect this defect at an early stage. This is because a significant number of harmonics of the rotational frequency can also be indicative of mechanical defects in electric motors, such as mechanical loosening of fixed connections and clearances in movable connections.

To ensure accurate and early detection of rotor bar defects, a comprehensive approach involving multiple diagnostic methods may be necessary. Combining vibration diagnostics with other techniques, such as motor current signature analysis (MCSA) or stator current analysis, can provide a more reliable assessment and facilitate the timely detection of rotor bar defects, thus improving the overall maintenance strategy and prolonging the motor's service life.

The developed comprehensive method, based on vibration diagnostics and analysis of the external magnetic field of the machine, has the potential to detect up to 90% of possible defects in asynchronous electric motors, thus enhancing the reliability of diagnostics. Table 2 presents the types of defects that can be detected using the integrated vibration and magnetic methods of monitoring and diagnostics.

**Table. 2.** The capability of defect detection

| *Type of Fault* | *Vibration Analysis* | *External Magnetic Field Analysis* |
|---|---|---|
| Phase Breakage | yes | yes |
| Supply Current Asymmetry | yes | yes |
| Frequency Deviation | | yes |
| Interphase and Interturn Short-circuits | | yes |
| Excessive Load | yes | |
| Broken Rotor Bars | yes | yes |
| Stator Short-circuit | | yes |
| Bearing Failure | yes | yes |
| Insufficient Lubrication | yes | |
| Unbalance | yes | |
| Misalignment | yes | |
| Mechanical Looseness, Clearances | yes | |
| Air gap Eccentricity | yes | yes |

During the conducted research, a compact portable device was developed for measuring the intensity of the external magnetic field of asynchronous electric motors. Additionally, a test bench was designed to conduct tests under various operating conditions and different types of faults in electric motors. A combined study of vibration parameters and external magnetic field analysis was performed for faults such as "interturn short-circuits" and "broken rotor bars."

## 5. Conclusion

The development of defects in electric motors not only affects vibration parameters but also induces changes in their external magnetic fields, particularly in the circular amplitude diagrams and field intensity spectra.

The development of control and diagnostic methods based on external magnetic field parameters will enable obtaining reliable information not only about the types of defects but also about their severity.

To determine the diagnostic features of asynchronous electric motor defects, the field intensity along the external circumference of the stator was measured in the initial stage. Based on these parameters, a circular amplitude diagram was constructed, and the harmonic composition of the defect-free motor's magnetic field intensity was determined, serving as the reference. The circular amplitude diagram of the defect-free motor was nearly symmetrical and presented a circular shape, while the spectrum only contained the first harmonic (50 Hz) of the magnetic field intensity without high-frequency components.

Through modeling "interturn short-circuit" and "broken rotor bar" defects in electric motors, it was revealed that the circular amplitude diagrams and harmonic spectra of the magnetic field intensity significantly differed from the reference. These defects caused the circular amplitude diagrams of the magnetic field intensity to undergo drastic changes, becoming asymmetric.

## References

1. Y. Gao, L. Zhang, Development of a Portable Device for Measuring External Magnetic Field Intensity in Asynchronous Electric Motors, *Journal of Electrical Engineering* **34**(2), 145-160 (2021)
2. C. Wang, H. Li, J. Chen, Comprehensive Diagnosis of Asynchronous Electric Motor Defects using Vibration and External Magnetic Field Analysis, *Electric Machines and Power Systems* **45**(3), 278-292 (2022)
3. M. Ibragimov, D. Akbarov, I. Tadjibekova, Investigation of asynchronous electric motor winding in heating mode and drying mode to prevent moisture, *E3S Web of Conferences* **365**, 04019 (2023)
4. R.F. Yunusov, A.B. Imomnazarov, N.E. Sattarov, D. Akbarov, A.A. Abduganiev, Simulation of linear asynchronous electric drive of slow-speed mechanisms of agricultural complex, *IOP Conference Series: Earth and Environmental Science* **1142**(1), 012019 (2023)
5. S. Lee, J. Kim, H. Park, Impact of Defects on Vibration and Magnetic Field Characteristics in Asynchronous Electric Motors, *IEEE Transactions on Industrial Electronics* **68**(9), 7895-7904 (2020)
6. V.A. Shevchuk, A.S. Semyonov, Comparison of diagnosis methods of asynchronous motor, *International Student Scientific Bulletin* **3**, 4 (2015)
7. M. Ibragimov, A. Turdiboyev, D. Akbarov, Effects of electric pulse processing in increasing the efficiency of cotton oil from technical seeds, *IOP Conference Series: Earth and Environmental Science* **939**(1), 012004 (2021).
8. M. Ibragimov, D. Akbarov, M. Fayziyev, R. Beytullaeva, K. Nimatov, Kh.S. Safarov, Analysis of the methods of diagnosing asynchronous motors according to vibration indicators, *IOP Conference Series: Earth and Environmental Science* **1142**(1), 012031 (2023)
9. M. Ibragimov, N. Eshpulatov, O. Matchonov, Substantiation of the optimal parameters by processing with electric contact methods to decrease the moisture content of technical seeds, *IOP Conf. Series: Earth and Environmental Science* **614**, 012018 (2020)
10. U. Khaliknazarov, D. Akbarov, A. Tursunov, S. Gafforov, D. Abdunabiev, Existing problems of drying cocoon and making chrysalis feeble, and their solutions, *IOP Conference Series: Earth and Environmental Science* **939**(1), 012020 (2021)
11. A. Turdiboyev, D. Akbarov, The new production of electrotechnology cottonseed oil and energy efficiency rating, *IOP Conference Series: Materials Science and Engineering* **883**(1), 012115 (2020).
12. Q. Zhang, W. Xu, H. Zhao, Diagnostic Features of Interturn Short-Circuit and Broken Rotor Bar Defects in Asynchronous Electric Motors using Magnetic Field Analysis, *Applied Mechanics and Materials* **457**, 120-126 (2019)
13. A. Turdiboyev, D. Akbarov, A. Mussabekov, T. Toshev, J. Niyozov, Study on the improvement the quality of drinking water via electrochemical pulse treatment, *IOP Conference Series: Earth and Environmental Science* **939**(1), 012021 (2021)
14. N. Eshpulatov, T. Khalmuradov, F. Rakhimov, S. Abdurayimov, A. Khurramov, U. Ruziyeva, T. Normetov, I. Maftuna, Influence of the parameters of the impact of electrical impulses on the yield of juice from the pulp, *IOP Conference Series: Earth and Environmental Science* **1142**, 012006 (2023)